

Large angular dispersion by a virtually imaged phased array and its application to a wavelength demultiplexer

M. Shirasaki

Fujitsu Laboratories Ltd., Optoelectronic Systems Laboratory, 4-1-1 Kamikodanaka, Nakahara-ku, Kawasaki, 211-88, Japan

Received September 29, 1995

A new scheme that shows large angular dispersion is proposed and demonstrated. The key idea to this method is a virtually imaged phased array (VIPA). The angular dispersion of a VIPA is 10–20 times larger than those of common diffraction gratings, which have blaze angles of ~ 30 deg. With the VIPA, wavelength demultiplexing for 10 channels with 0.8-nm spacing is achieved. Low polarization-state dependence (~ 0.1 dB) is also confirmed. © 1996 Optical Society of America

Optical multiplexing/demultiplexing is a critical function in high-density wavelength-division multiplexing systems for ~ 1 -nm channel spacing. To obtain this function for a multichannel system by using wavelength splitters such as Fabry–Perot or Mach–Zehnder interferometers, one has to cascade a number of those splitters. A diffraction grating provides a much simpler means of decomposing light into many wavelengths at one time.^{1,2} For this purpose, however, common diffraction gratings have some disadvantages, i.e., polarization-state dependence of the diffraction efficiency and insufficient angular dispersion. Because of this low dispersion, the multiplexer/demultiplexer for dense channels is not compact, and its characteristics are sensitive to misalignment.

Here a novel scheme that shows large angular dispersion is proposed and demonstrated. The key idea to this method is a virtually imaged phased array (VIPA). Application of the VIPA to an optical demultiplexer is confirmed. The VIPA has the following advantages over diffraction gratings: large angular dispersion (10–20 times larger than common gratings, which have ~ 30 -deg blaze angles); low dependence of the input polarization state; simple structure and low cost; and compactness.

The VIPA employs a thin plate of glass and semi-cylindrical lens (C lens), as shown in Fig. 1. The input light is line focused with the semi-cylindrical lens into the glass plate. Then the collimated light emerges on the other side of the plate, where the light propagates at the angle that varies as the wavelength of the light changes.

The details of the VIPA structure are shown in Fig. 2. One side of the glass plate is coated with a high-reflection film ($\sim 95\%$ reflectivity or greater). The other side is coated with a 100%-reflection film except in the window area, which is antireflection (AR) coated. The input light enters the plate through the window and is line focused onto the other surface of the plate with a semi-cylindrical lens (C lens). Here the center axis of the input light to the surface has a small incident angle θ . Note that θ is the incident angle inside the plate and that the incident angle from the air to the plate is $\sim n$ times larger because of refraction (n is the refractive index of the plate, and $n = 1.5$ for glass). This refraction is ignored in Fig. 2

for simplicity. 5% of the input light passes through the surface and diverges after the beam waist. 95% of the input light is reflected and, after the second reflection, hits the same surface but is displaced by an amount d . Then 5% of the light passes through the surface. In a similar way, the light after the plate is split into many paths with a constant separation d . It is easily understood that the beam shape in each path forms so that the light diverges from a virtual image of the beam waist. The virtual images of the beam waist are located with constant spacing $2t$ (t is the thickness of the plate) along the line that is normal to the plate. The positions of the beam waists in the virtual images are self-aligned, and there is no need to adjust individual positions. Then all the beams interfere and form collimated light, where the light propagates in a direction that is determined by an angle similar to the Bragg angle of a diffraction grating.

The spacing of the light paths is $d = 2t \sin \theta$, and the difference in the path lengths between adjacent beams is $2t \cos \theta$. The angular dispersion is proportional to the ratio of these two numbers, which is $\cot \theta$. The angular dispersion after the plate is $\sim n$ times larger because of refraction. Thus the effective factor that determines the dispersion is approximately $n \cot \theta$.

One way in which a VIPA is different from a diffraction grating is that the field magnitudes of the virtual images decay exponentially as the number of reflections increases. In a diffraction grating the field magnitude on the grating surface is determined by the input beam profile and is often Gaussian. The decay rate in one round trip in a VIPA is the square root of the reflectivity, which is ~ 0.975 when the reflectivity

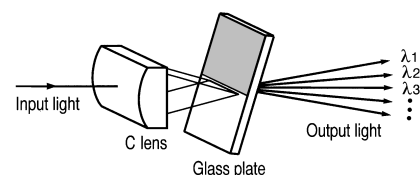


Fig. 1. Schematic of wavelength decomposition with the VIPA. The input light is line focused with a semi-cylindrical lens (C lens) into a thin plate of glass. Collimated light emerges at the output, and the output angle varies as the wavelength changes.

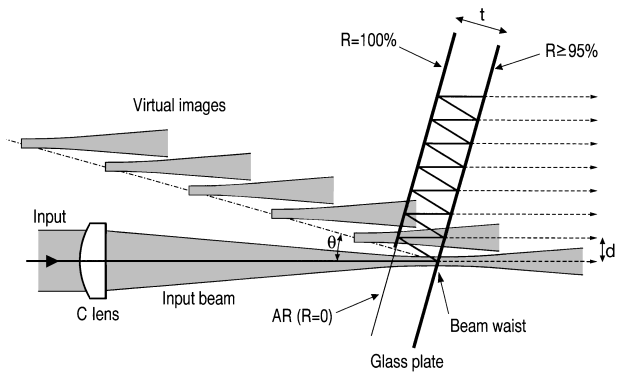


Fig. 2. Details of the VIPA structure. A glass plate ($\sim 100 \mu\text{m}$ thick) has 95%-reflection coating on the right surface and 100%-reflection coating on the left surface. There is a window area on the left surface, which has antireflection coating (AR) instead of 100%-reflection coating. The glass plate produces many beams diverging from individual virtual images of the beam waist. These beams interfere and form collimated light.

is 95%. Under the conditions that the reflectivity has no phase and does not vary in the range of the incident angle, the beam profiles in all the light paths are the same because they are the virtual images. Assuming that the field magnitude in a beam is constant around the output peak direction, the output field traveling in the direction of angle $\Delta\phi$ ($\Delta\phi$ is the small deviation, in radians, from the Bragg angle) is proportional to $1/[1 - \exp(-\alpha + ikd\Delta\phi)] \approx 1/(\alpha - ikd\Delta\phi)$. Here $\exp(-\alpha)$ is the decay rate in the VIPA and $k = 2\pi/\lambda$ (λ is the wavelength). The approximation is valid for small α and small $kd\Delta\phi$. Thus the far-field pattern of the output light is Lorentzian.

It is of interest to evaluate the coupling efficiency from the Lorentzian output to a Gaussian mode. The beam profile in the direction perpendicular to the plane of Fig. 2 is assumed to be Gaussian. Then the coupling efficiency is determined by a two-dimensional model in the plane of Fig. 2. When the output light from the VIPA is focused onto a Gaussian mode with a lens, the coupling efficiency is calculated from the square of the overlap integral between the Gaussian field and $\exp(iky\Delta\phi)/(\alpha - ikd\Delta\phi)$. Here y is the lateral position of the lens. Numerical simulation showed that the coupling efficiency was as high as 80% when the lens position and the focal length were optimized.

The VIPA is essentially polarization insensitive. Polarization dependence of a VIPA appears only if the complex reflectivities of the reflection films have polarization dependence in either amplitude or phase. But their polarization dependence can be ignored for a small incident angle below 10 deg.

The parameters used in the following experiments, for the 1.55- μm wavelength range, are $t = 100 \mu\text{m}$, $\theta = 6.4$ deg, and $d = 22.4 \mu\text{m}$. Thus the factor $n \cot \theta$ described above is 13.4. A similar factor for a diffraction grating is $2 \tan(\text{blaze angle})$, and this factor for a common blaze angle of ~ 30 deg is ~ 1 . Thus the angular dispersion of the VIPA is much larger than those of the gratings. One important design issue in a VIPA is to ensure that the input light passes through

the window area and that the light is incident upon the 100%-reflection area after the first reflection. This requirement determines the minimum angle θ . When the beam thickness at the beam waist is $10 \mu\text{m}$, the beam thickness on the window, which is $\sim 100 \mu\text{m}$ apart from the beam waist in the glass, is $12 \mu\text{m}$. Then θ must be larger than 3.5 deg, and the above θ satisfies this condition. A sharp boundary is required between the window and the 100%-reflection area. To make a sharp boundary, first the entire surface was coated with a 100%-reflection film and then the film was removed in the window area. Finally, a glass chip was fastened over the window with index-matching glue. This chip had an antireflection coating upon the external facet.

In the first experiment the angular dispersion of the VIPA was measured. The input light from a wavelength-tunable laser diode in the 1.55- μm range was introduced through a single-mode fiber and collimated with a plano-convex lens (radius of curvature 3 mm), as shown in Fig. 3. The light was then line focused with a semicylindrical lens (C lens) having a 3-mm radius of curvature. First it was confirmed that the output light from the glass plate was well collimated. The beam diameter measured at a distance of 20 cm from the glass plate was ~ 0.6 mm. Next the output angle ϕ was measured and is shown in Fig. 4.

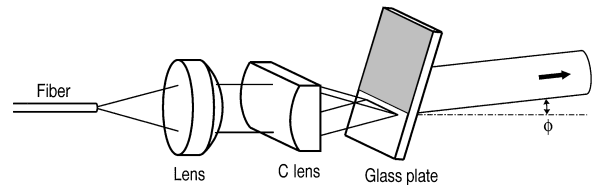


Fig. 3. Experimental setup for the measurement of angular dispersion. The input light from a single-mode fiber is collimated and line focused with a semicylindrical lens (C lens). The output light propagates at angle ϕ .

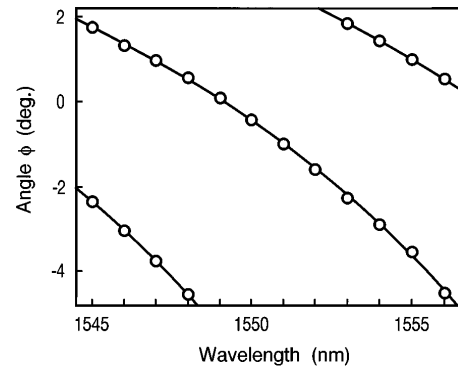


Fig. 4. Relation between angle ϕ and wavelength. The dispersion is 0.4–0.8 deg/nm, and the spacing from one wavelength to the next is 8 nm.

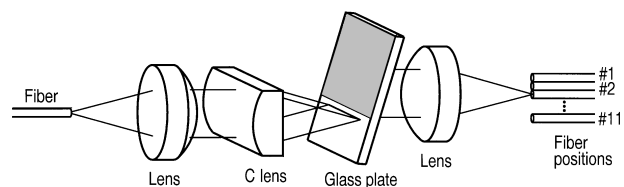


Fig. 5. Schematic of the wavelength demultiplexer. The collimated light from the glass plate is focused into the output fiber.

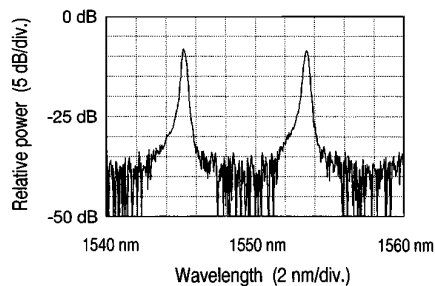


Fig. 6. Transmission spectrum through fiber #5 (Fig. 7). 3- and 20-dB bandwidths are 0.3 and 1.5 nm, respectively.

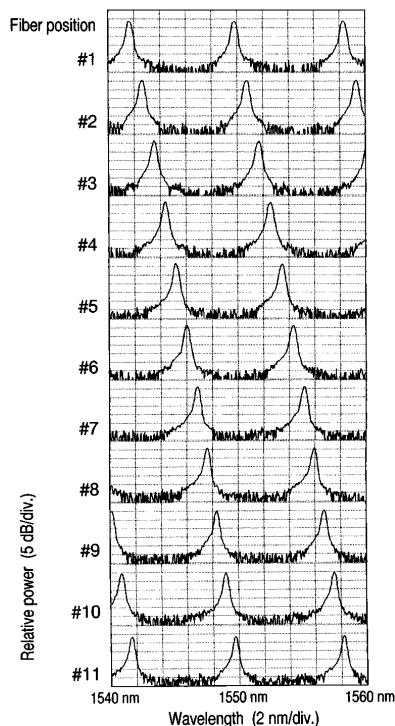


Fig. 7. Transmission spectra for the 11 fiber positions. The characteristics for a 10-channel wavelength demultiplexer with 0.8-nm channel spacing are obtained.

When the wavelength changes, ϕ changes sensitively. It appears that the curve is not linear and that the angular dispersion $|d\phi/d\lambda|$ is larger at smaller ϕ . This is because the change of ϕ is not small enough to be neglected; then the effective factor for the dispersion becomes $n \cot(\theta + \phi/n)$. The angular dispersion varies from 0.4 to 0.8 deg/nm as a function of ϕ , not of the wavelength. For $\phi = 0$ the angular disper-

sion is ~ 0.5 deg/nm, and this value is in good agreement with the theoretical value $n \cot \theta / \lambda$ in radians per nanometer.

Using this large angular dispersion, I constructed a wavelength demultiplexer as shown in Fig. 5. The focal length of the output lens was 20 mm, and there were 11 output fiber positions that had a 110- μm spacing. The output fiber had a 62.5- μm -diameter step-index core. First, the transmissivity from the input fiber to the output fiber #5 was measured with a LED light source and an optical spectrum analyzer. The result is shown in Fig. 6. The spacing between the transmission peaks is ~ 8 nm, corresponding to the thickness of the glass plate. The 3- and 20-dB transmission bandwidths are ~ 0.3 nm and ~ 1.5 nm, respectively. The polarization-state dependence of the transmissivity at the peak wavelength was measured to be ~ 0.1 dB. The transmission spectra for 11 fiber positions are shown in Fig. 7. The change of spectra corresponds to an angular dispersion of 0.4 deg/nm. This figure shows that the obtained characteristics are suitable for a 10-channel wavelength-division multiplexing system with 0.8-nm spacing. Inasmuch as the lens parameters are not optimized in this experiment, the loss and the cross talk from the neighbor channel are theoretically limited to 1.9 and -35 dB, respectively. In the demultiplexing experiment the effective size of the glass plate is 1 mm \times 1 mm \times 0.1 mm. Thus the device can potentially be packaged within a 1–2-mm-diameter area.

A scheme for large angular dispersion has been proposed and demonstrated. Its application to a wavelength demultiplexer was also demonstrated. Large angular dispersion of 0.4–0.8 deg/nm was observed, and demultiplexing of 10 wavelengths with 0.8-nm spacing was successfully achieved with a polarization-state dependence of 0.1 dB. The wavelength range for demultiplexing was limited to 8 nm by the output in the next order. Reducing the thickness of the glass plate to 50 μm will double the wavelength range to 16 nm.

The author thanks M. Seino and T. Nakazawa for help with the fabrication and N. Fukushima for help with the measurements.

References

1. J. Lipson, W. J. Minford, E. J. Murphy, T. C. Rice, R. A. Linke, and G. T. Harvey, *J. Lightwave Technol.* **LT-3**, 1159 (1985).
2. D. R. Wisely, *Electron. Lett.* **27**, 520 (1991).